Journal of Optoelectronics and Advanced Materials Vol. 2, No. 5, 2000, p. 481-486

Section 1: Single crystal materials

THERMO-HYDRODYNAMIC TRANSIENT MODELING OF VERTICAL BRIDGMAN GROWTH

C. Stelian[a], J. L. Plaza[b], F. Barvinschi[c], T. Duffar[d], J. L. Santailler[d], E. Dieguez[b], I. Nicoara[a]

[a]Departament of Physics, West University of Timisoara, Bd.V.Parvan, No.4, 1900 Timisoara, Romania
[b]DFM/LCC, Universidad Autonoma de Madrid, E-28049 Madrid, Spain
[c]Technical University of Timisoara, Dept.of Physics, P-ta Horatiu, No.1, 1900 Timisoara, Romania
[d]CEA/CEREM/DEM, Commissariat à l'Energie Atomique, 17, Avenue des Martyrs, 38054 Grenoble, France

Velocity and temperature fields in the growth of semiconductor by the vertical Bridgman method are studied by numerical modeling using the finite element code FIDAP. A free surface model is applied for the description of the transient process. Using the numerical results the solid-liquid interface evolution with time is discussed.

Keywords: Vertical Bridgman growth, Numerical simulation, Transient analysis, Interface deflection

1. Introduction

The vertical Bridgman method is often used for the growth of semiconductor single crystals. Numerical studies have been dedicated to the analysis of the fluid flow and heat transfer, but they generally use an idealized quasi-steady model for the system [1-3].

In the present paper the finite element software FIDAP is used to perform a transient analysis of the vertical Bridgman process. The model system consist in GaSb grown in a boron nitride crucible. It is known that the heat transfer and melt convection during the growth process influence the interface position, velocity and shape, then quality of the crystal. For this reason the attention is focused on the coupled heat and momentum transport effects on the interface. The effect of the latent heat release on the interface deflection is also discussed.

2. Model description

2.1 Growth configuration

We consider the vertical Bridgman configuration [4] for the growth of GaSb. The charge is contained in a boron nitride crucible, which is moved into a furnace which has a tapered heating element. The schematic diagram of the system and the mathematical domain of simulation are presented in Fig. 1. The physical properties of GaSb, BN and other input parameters are tabulated in Table 1.

2.2 Governing equations

The dimensionless equations of continuity, momentum and transport of heat, in the Boussinesq approximation, are:

- Mass-conservation equation:

$$\nabla(\rho\vec{u}) = 0 \tag{1}$$

- Momentum equation:

$$\sqrt{Gr}\left(\frac{\partial\vec{u}}{\partial t} + \vec{u}\nabla\vec{u}\right) = -\nabla p + \nabla\vec{u} + \sqrt{Gr}\,T \tag{2}$$

- Heat transfer equation:

$$\sqrt{Gr}\,\mathrm{Pr}\left(\frac{\partial T}{\partial t} + \vec{u}\nabla T\right) = \nabla^2 T \tag{3}$$

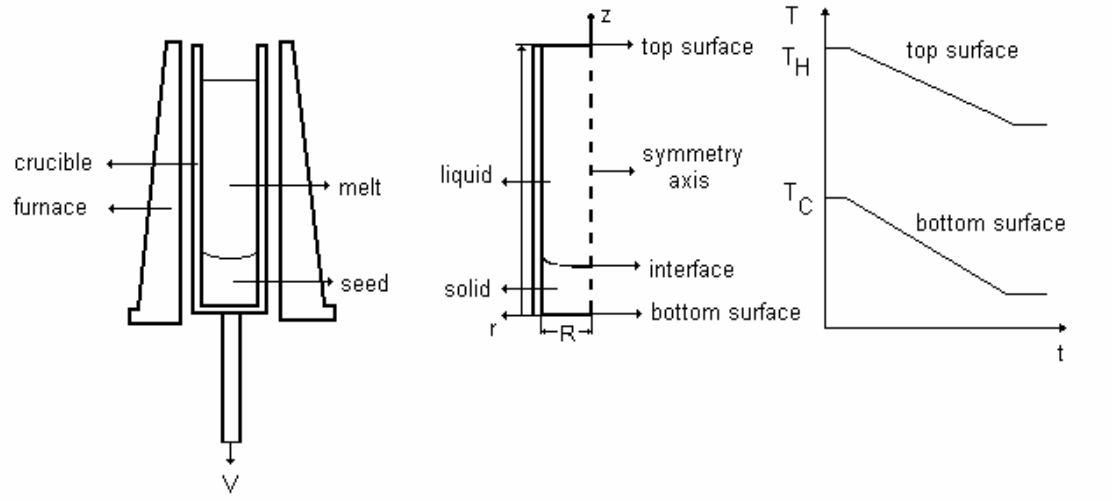

(a) (b)

Fig. 1. Schematic sketch for the vertical Bridgman system: (a) model of the furnace (b) domain of the simulation and temperature profile.

The dimensionless variables are defined by:

$$t = \tilde{t}\,U/R, \quad \nabla = R\tilde{\nabla}, \quad u = \tilde{u}/U, \quad p = \tilde{p}/\rho U^2, \quad T = (\tilde{T} - \tilde{T}_C)/(\tilde{T}_H - \tilde{T}_C) \tag{4}$$

where the tilde denotes the corresponding dimensional quantity.
$U = \sqrt{\beta_T \Delta T g R}$ is the characteristic speed of the flow driven by buoyancy forces. The radial thermal gradient at the solid/liquid interface is:

$$\Delta T = fG_T \tag{5}$$

where f is the interface deflection, calculated by [5]:

$$f = \frac{R}{2}\left[\frac{k_L}{k_S}\left(\frac{k_S R^2 + k_a(2R+e)e}{k_L R^2 + k_a(2R+e)e}\right) - 1\right] \tag{6}$$

e being the crucible thickness.

The Grashof number (Gr) and the Prandtl number (Pr) are defined as follows:

$$Gr = \rho^2 \beta_T \Delta T g R^3/\mu^2, \ \mathrm{Pr} = \mu c_P/k \tag{7}$$

Table 1

Physical properties of GaSb, BN and other input parameters	
Density	$\rho_S = 5.6\times10^3 kg\cdot m^{-3}$
	$\rho_L = 6.06\times10^3 kg\cdot m^{-3}$
	$\rho_C = 1.9\times10^3 kg\cdot m^{-3}$
Thermal conductivity	$k_S = 6.43 W\cdot m^{-1}K^{-1}$
	$k_L = 10.24 W\cdot m^{-1}K^{-1}$
	$k_C = 20.6 W\cdot m^{-1}K^{-1}$
Specific heat	$c_{PS} = 0.3\times10^3 J\cdot kg^{-1}K^{-1}$
	$c_{PL} = 0.33\times10^3 J\cdot kg^{-1}K^{-1}$
	$c_{PC} = 1.85\times10^3 J\cdot kg^{-1}K^{-1}$
Heat of fusion	$\Delta H = 3.13531\times10^5 J\cdot kg^{-1}$
Thermal diffusivity	$\alpha = 5.1\times10^{-6} m^2\cdot s^{-1}$
Thermal expansion coefficient	$\beta_T = 9.6\times10^{-5} K^{-1}$
Viscosity of melt	$\mu = 2.242\times10^{-3} kg\cdot m^{-1}s^{-1}$
Melting point	$T_S = 979 K$
Furnace axial temperature gradient	$G_T = 5\times10^3 K\cdot m^{-1}$
Crystal radius	$R = 5\times10^{-3} m$
Crucible radius	$R_C = 6\times10^{-3} m$
Crucible length	$L = 5\times10^{-2} m$
Translation rate	$V = 7\times10^{-6} m\cdot s^{-1}$
Bottom temperature	$T_C^{t=0} = 929 K$
Top temperature	$T_H^{t=0} = 1179 K$

The boundary conditions for the temperature along the bottom and top surface are given by:

$$\tilde{T}'_C(t) = \tilde{T}_C - |G_T|_S\, l \tag{8}$$

$$\tilde{T}'_H(t) = \tilde{T}_H - |G_T|_L\, l \tag{9}$$

where $l = Vt$ is the crucible translated at time t, $|G_T|_S$ is the axial temperature gradient in the solid and $|G_T|_L$ is the axial temperature gradient in the liquid.

The heat fluxes at the symmetry axis and at the external surface of the crucible are:

$$\left.\frac{\partial T}{\partial r}\right|_{r=0} = 0 \tag{10}$$

$$\left.\frac{\partial T}{\partial r}\right|_{r=R_C} = 0 \tag{11}$$

The energy balance across the solid-liquid interface is given by:

$$(K\nabla T|_S - \nabla T|_L)\vec{n} = \rho_S V\Lambda \tag{12}$$

where $K = k_S / k_L$ is the ratio of thermal conductivities of solid to melt, $\vec{n}$ is the unit vector normal to the solid-liquid interface and $\Lambda = \frac{R\Delta H}{k_L(\tilde{T}_H - \tilde{T}_C)}$ is the adimensional quantity for the heat of fusion.

For the velocity field a no-slip conditions is used on the solid inner surfaces of the melt:

$$\vec{v} = 0 \tag{13}$$

and the condition:

$$v_z = 0 \tag{14}$$

is imposed on the upper surface of the melt.

The symmetry condition along the centerline of the system is:

$$v_r = 0 \tag{15}$$

3. Results and discussion

The non-linear set of equations is solved using the finite element code FIDAP. The 2D –mesh of the physical domain is shown in Fig. 2. It contains 2880 quadrilaterals elements and the meshing density is increased near the solid-liquid interface.

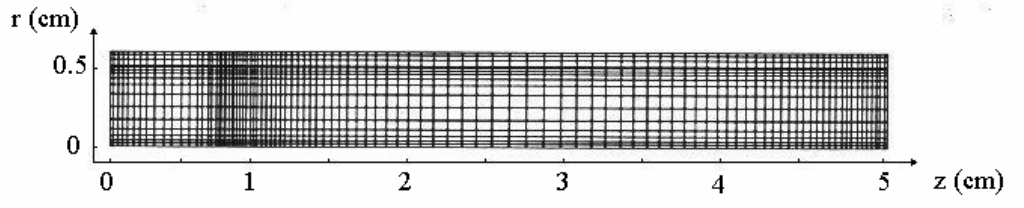

Fig. 2. Computational mesh.

In the first stage of modeling the thermal convection and the heat transport when the solid-liquid interface entity is fixed, are simulated. The results for the temperature and flow fields are used as initial conditions for the steady-state simulation with a free boundary. In this method, the solid-liquid interface is defined as a free surface and the mesh is deformed in order to position the nodes on the isotherm corresponding to the melting temperature. Fig. 3 shows the mesh deformation in the liquid and corresponding crucible domains. As seen in Fig. 4, a single torroidal cell flow is observed near the interface. The results is obtained for a Grashof number Gr=4350. The maximum value for the melt velocity is $u_{max} = 1.3 \cdot 10^{-5}$ m/s. The isotherms are distorted near the solidification interface only, with a concave shape seen from the liquid.

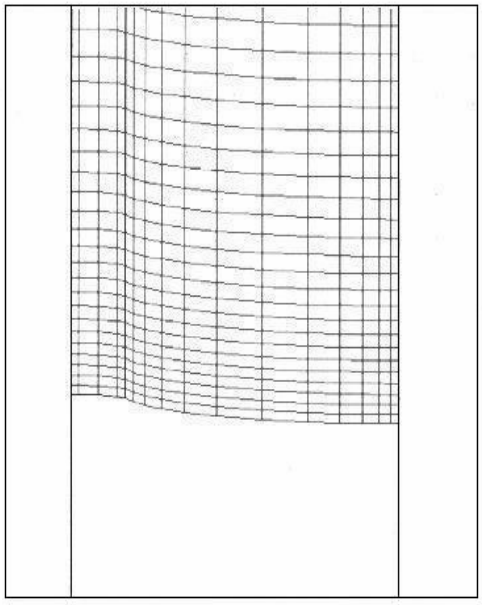

Fig. 3. Mesh deformation.

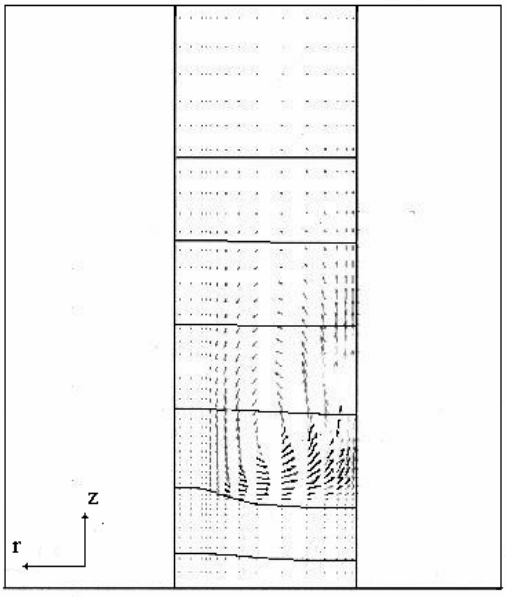

Fig. 4. Flow pattern and isotherms (12.5K increment) near the interface.

In the second stage of modeling, the transient analysis of the growth process is performed with the steady-state results as initial conditions. In the initial transient of solidification, an increase of the interface deflection is observed. This phenomenon is due to the latent heat generated by the solidification process and depends on the growth rate. The solid-liquid interface position and shape at several stages of the pulling process are shown in Fig. 5. The interface deflection increases from f = 0.39 mm at the beginning to f = 0.57 mm at the end of the initial transient growth. This effect is explained by the evolution of the growth rate. As it is shown in the Fig. 6, an initial transient of the growth rate, measured as the interface velocity on the symmetry axis, is observed. This phenomenon has been investigated in the references [6,7], where an exponential law has been proposed for the growth rate:

$$V(t)=V_f-(V_f-V_i)\exp(-\frac{t}{\tau}) \tag{16}$$

V_i and V_f are respectively the initial and the final growth rates. From Fig. 6 it comes the time constant τ=220 s.

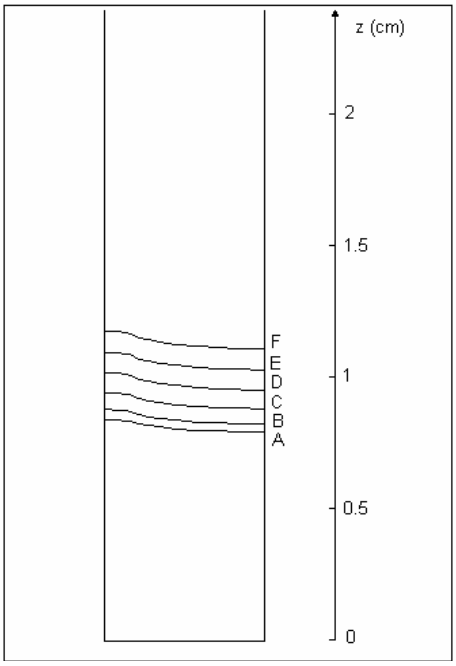

Fig. 5. Solid-liquid interface shape at several stages of the growth process; the interface deflection increase from: f (A) = 0.39 mm at t = 25 s, to f (F) = 0.57 mm at t = 650 s.

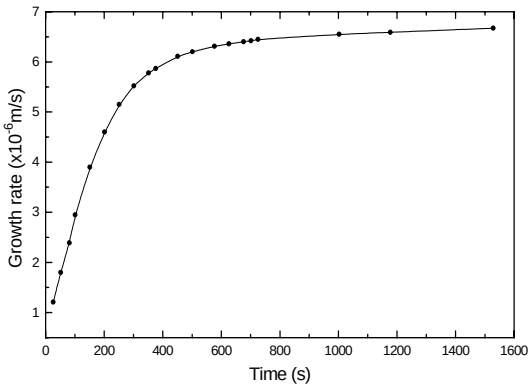

Fig. 6. Growth rate versus time at a constant translation rate V=7·10^{-6} m/s.

Fig. 7 and 8 shown the same results for a translation rate V=7·10^{-7} m/s. The effect of the latent heat produced during the solidification process is smaller and no increase of the interface deflection in the initial transient can be observed.

According to [7], the time constant τ depends on the thermal coupling between the furnace and the charge and the latent heat release. However it appears that τ is not changed when the growth rate is ten times lower. It can be concluded that the latent heat effect on the transient is negligible in the frame of the present study. Indeed τ is of the order of magnitude of the heat transfer along the sample

$\tau \approx \frac{L^2}{\alpha} \approx 300\ s$. It is also in agreement with the published values [7].

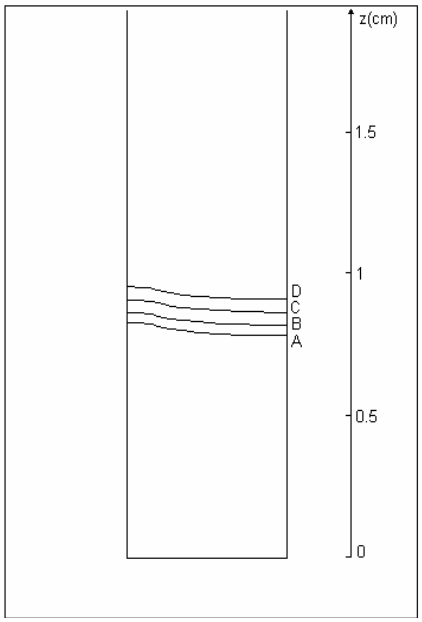

Fig. 7. Solid-liquid interface shape at several stages of the growth process; the interface deflection is: f (A) = 0.38 mm at t = 1 s, and f (D) = 0.38 mm at t = 1950 s.

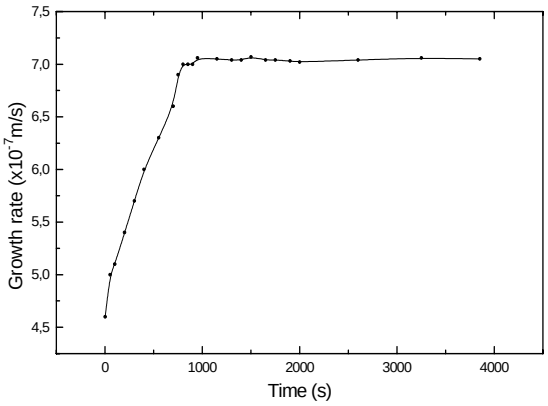

Fig. 8. Growth rate versus time at a constant translation rate $V=7\cdot10^{-7}$ m/s

4. Conclusions

The effect on the interface velocity and shape of the heat transfer, melt convection and latent heat release has been studied with the help of numerical simulation. A transient axi-symmetric model was solved by the finite element method using a deformable mesh tracking the solidification isotherm.

At the beginning of the solidification an initial transient of the growth rate is observed. The time constant of this transient is in agreement with published values and with the order of magnitude of the heat transfer duration along the sample. It appears that the length of the transient does not depend on the cooling velocity, and then the effect of latent heat is negligible for the parameters used in this study.

Considering the solid-liquid interface deflection it is shown that it does not change during the initial transient when a slow cooling rate is applied. For a cooling rate ten times higher, the interface deflection increases by 50 % during the initial transient. This is attributed to the latent heat release which is not negligible. The deflection increases because there is an increasing heat flux toward the crucible.

These results are in good qualitative and quantitative agreement with the published results and the numerical model can reasonably be considered as reliable. It will be used for in-depth study of the thermal, hydrodynamic and solutal interactions in vertical Bridgman growth.

References

[1] P. M. Ardonato, R. A. Brown, J.Crystal Growth, **80,** 177(1987).
[2] M. C. Liang, C. W. Lan, J. Crystal Growth, **167**, 325(1996).
[3] C. Barat, T. Duffar, P. Dusserre, J. P. Garandet, Cryst. Res. Technol., **34**, 4, 453(1999).
[4] C. Barat, PhD thesis, Universite de Rennes (1995).
[5] C. Barat, T. Duffar, J. P. Garandet, J. Crystal Growth **194,** 151(1998).
[6] T. W. Fu, W. R. Wilcox, J. Crystal Growth **51,** 557(1981).
[7] C. A. Wang, A. F. Witt, J. R. Carruthers, J. Crystal Growth **66,** 303(1984).